PASSIVE MILLIMETER-WAVE IC COMPONENTS MADE OF INVERTED STRIP DIELECTRIC WAVEGUIDES

T. Itoh* and R. Rudokas
Department of Electrical Engineering and
Coordinated Science Laboratory
University of Illinois at Urbana-Champaign
Urbana, Illinois 61801

Abstract

Unique directional couplers and ring resonators for millimeter-wave IC's were created from the inverted strip dielectric waveguide. They were tested in the 75-80 GHz range, and the agreement between the theoretical and experimental results was found to be quite satisfactory.

Introduction

A number of different waveguide structures are currently available for millimeter-wave integrated circuits.[1-5] Recently, a novel structure, inverted strip dielectric (IS) waveguide, has been proposed and analyzed.[6] The purpose of the present paper is to report the theoretical and experimental investigations on several millimeter-wave passive IC components made from the IS waveguide. They are the distributed-type directional couplers, the beam-splitter type couplers, and the ring resonators.

Review of "IS" Waveguide

Let us first briefly describe the IS guide, the cross section of which is shown in Figure 1b. A teflon strip (1.58 mm thick) is sandwiched between the ground plane and the fused quartz plate (1.58 mm thick). Since the dielectric constant of the quartz plate ($\varepsilon_2 = 3.8$) is higher than that of the teflon ($\varepsilon_1 = 2.1$), most of the wave energy propagates in the former. In addition, the teflon strip provides a lens effect in the sideward direction, resulting in the energy concentration in the quartz plate region immediately above the strip. The principal advantage of the IS guide is that the conductor loss can be greatly reduced because the energy flow is not at the conductor surface and yet the conducting ground plane is convenient as a heat sink and as a dc bias return for the solid state devices which may be mounted in the IS guide. Since an extensive analysis of IS guides is found in 6, only the basic steps will be described here. The analysis is based on the concept of the effective dielectric constant. If the regions I, II, and III are individually infinitely wide in the x-direction, each becomes a slab waveguide whose transverse wave number k_y or $\bar{k}_y$ can be easily computed by solving simple eigenvalue equations.[7] The effective dielectric constants in Region II and Regions I and III are defined by

$$\varepsilon_{e2} = \varepsilon_2 - \left(\frac{k_y}{k_0}\right)^2 , \varepsilon_{e1} = \varepsilon_{e3} = \varepsilon_2 - \left(\frac{\bar{k}_y}{k_0}\right)^2 , \varepsilon_{e2} > \varepsilon_{e1} \qquad (1)$$

and may be considered as those of the hypothetical medium in which the phase velocity of the plane wave is identical to that of the surface wave in the original structures.

Having determined these quantities, one replaces I, II and III by the vertical slab media with the corresponding effective dielectric constants, and the eigenvalue equation in the x-direction for this new slab structure is solved. The obtained propagation constant is assumed to be that of the original IS guide.

*He is now at Stanford Research Institute, Menlo Park, California 94025

Beam-Splitter Type Coupler

The cross coupler shown in Figure 1 operates on the principle of the optical beam splitter. A simple approximate analysis is presented, which is expected to give a first-order estimate of the coupling factor.

The coupler consists of two perpendicularly intersecting IS guides. The teflon strip has a gap of width s at the intersection. The orientation of the gap is 45 degrees with the four arms of the coupler. The effective dielectric constant of this gap portion is therefore ε_{e1} (corresponding to the quartz plate floating above the ground plane). On the other hand, in the regions where teflon is present, it is ε_{e2}.

Within the first-order approximation, the phase front of the dominant mode of the IS guide is similar to that of a plane wave. For a wave incident along arm 1, the incident angle at the junction is 45 degrees from the normal to the interface between the media with ε_{e1} and ε_{e2} (see Figure 1c and Figure 2). The reflected wave makes 45 degrees from the normal, resulting in the coupling into arm 3. With the help of Figure 1c, the power reflection coefficient can be calculated[8]

$$|\rho|^2 = \frac{\left(\alpha - \frac{1}{\alpha}\right)^2 \tan^2(k_0 sp\sqrt{\varepsilon_{e1}/2})}{4 + \left(\alpha + \frac{1}{\alpha}\right)^2 \tan^2(k_0 sp\sqrt{\varepsilon_{e1}/2})} \qquad (2)$$

where

$$\alpha = q/p, p = \sqrt{2 - \left(\frac{\varepsilon_{e2}}{\varepsilon_{e1}}\right)} , \quad q = \sqrt{\frac{\varepsilon_{e2}}{\varepsilon_{e1}}}$$

k_0 = free space wavenumber .

Figure 2 shows the experimental results in which the coupling factor was compared with the computed values. The agreement is quite reasonable. The insertion loss was obtained by comparing the total loss from terminals 1 to 2 with the loss of a straight section of IS guide of identical length. Figure 3 shows an actual view of the cross coupler.

Distributed-Type Directional Coupler

This coupler shown in Figure 4 consists of a coupled IS guide and four connecting IS guides. Note again that the actual wave propagation takes place in the quartz plate and that the role of the teflon strip is to create the guiding pattern. When the coupling is not too strong, the total coupling length L is given by[9]

$$L = \frac{\pi}{k_{ze} - k_{z0}} \qquad (3)$$

where k_{ze} and k_{z0} are the propagation constants of the even and odd modes of the coupled IS guide. The ratio of the power output from arms 2 and 3 is given by

$$\frac{P_3}{P_2} = \tan^2 \frac{\pi \ell}{2L} \quad . \tag{4}$$

When the coupler length ℓ is chosen to be L/2, a 3 dB coupler may be obtained. Theoretical and experimental results of a prototype coupler are shown in Figure 5. If the actual ℓ is used in the computation, the difference beween the measured and computed P_3/P_2 values is rather large. However, this choice of ℓ ignores the coupling between neighboring connecting arms. The extra coupling effects may be represented by a hypothetical extension of ℓ. The effective length $\bar{\ell}$ may be defined as

$$\bar{\ell} = \ell + \frac{\Delta\theta}{\pi} L \tag{5}$$

$$\Delta\theta = 2 \int_{z'}^{z''} [k_{ze}(z) - k_{z0}(z)] \, dz \tag{6}$$

where the integration must be carried out in the axial (z) direction of the coupler. z' corresponds to the junction between the coupler and the connecting arm, and z" is the z value beyond which the coupling between the arms is negligible and $k_{ze}(z)$ is practically identical to $k_{z0}(z)$. The factor 2 in (6) accounts for the couplings between the arms on both sides of the coupler. If this "effective ℓ" is used, the agreement between the theoretical and experimental results becomes much closer. The directivity of the guide was found to be more than 20 dB through the frequency band tested (75-80 GHz).

Ring Resonator

The photo of the ring resonator is shown in Figure 6. The resonant guide wavelength is obtained from

$$n\lambda = 2\pi\bar{r} \quad , \quad n = 1,2, \ldots \tag{7}$$

where $\bar{r}$ is the effective radius of the ring and is chosen to be

$$\bar{r} = \sqrt{ab}$$

if the maximum and minimum radii, a and b, are close to each other. If one assumes the guide wavelength in the ring resonator is identical to that in the straight IS guide, the resonant frequency is obtained from the dispersion relation. Note that this assumption is valid when the radius of curvature is relatively large. The measured frequency response of the ring resonator is shown in Figure 7. The computed resonance frequencies are also indicated. In the actual experiment, the input and output terminals are placed 90 degrees apart. The odd order (n:odd) resonances are not strongly coupled to the output terminal, because the odd orders have a node in the standing wave 90 degrees away from the excitation arm. The small peaks in the curve around 75.5, 77.0, and 78.5 GHz could be an indication of this phenomenon. The even-order resonances were strongly detected. The agreement between the computed and the measured resonances is somewhat poor, although the general nature of the curve is quite satisfactory. Note that, in the measurements, the coupling gaps between the resonator and the terminals are quite small. This tight coupling may have caused the shift of resonances.

Conclusions

Three passive components for the millimeter-wave IC have been developed using the inverted strip dielectric waveguide. Satisfactory agreement between the design theory results and the measured data was obtained.

References

1. M. V. Schneider, "Millimeter-wave integrated circuits," IEEE MTT Symposium, Boulder, Colorado, pp. 16-18, June 1973.
2. E. J. Denlinger, J. Rosen, E. Mykietyn and E. C. McDermott, "Microstrip varactor-tuned millimeter wave IMPATT diode oscillators," IEEE MTT Symposium, Palo Alto, California, pp. 266-267, May 1975.
3. H. Jacobs and M. M. Crepta, "Electronic phase shifter for millimeter-wave semiconductor dielectric integrated circuits," IEEE Trans. Microwave Theory Tech., vol. MTT-22, no. 4, pp. 411-417, April 1974.
4. R. M. Knox and P. P. Toulios, "A V-band receiver using image line integrated circuits," Proc. National Electronics Conf., vol. 27, pp. 489-492, October 1974.
5. W. McLevige, T. Itoh and R. Mittra, "New waveguide structures for millimeter-wave and optimal integrated circuits," IEEE Trans. Microwave Theory Tech., vol. MTT-23, no. 10, pp. 788-794, October 1975.
6. T. Itoh, "Inverted strip dielectric waveguide for millimeter-wave integrated circuits," to appear in IEEE Trans. Microwave Theory Tech., vol. MTT-24, no. 11, (special issue on Millimeter Waves), November 1976.
7. R. E. Collin, Field Theory of Guided Waves. New York, New York: McGraw-Hill, 1960.
8. S. Ramo and J. Whinnery, Field and Waves in Modern Radio. New York: Wiley, 1953.
9. K. Kurokawa, An Introduction to the Theory of Microwave Circuits. New York, New York: Academic Press, 1969.

Acknowledgment: The work presented here was supported in part by the Joint Services Electronics Program DAAB07-72-C0259 and in part by US Army Research Office DAHC04-74-G0113.

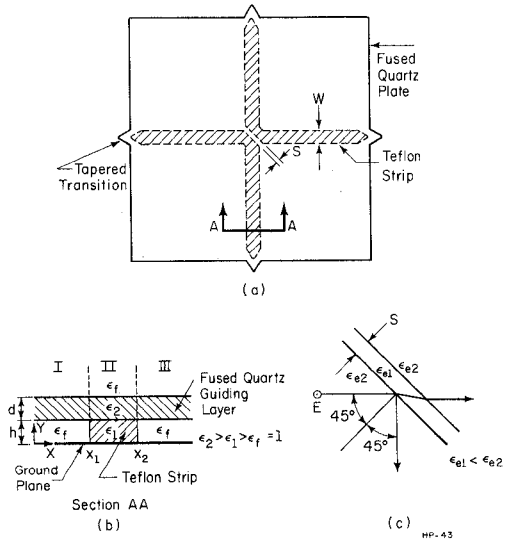

Fig. 1. Beam splitter type directional coupler: (a) top view, (b) cross section of one of the arms, (c) equivalent structure at junction.

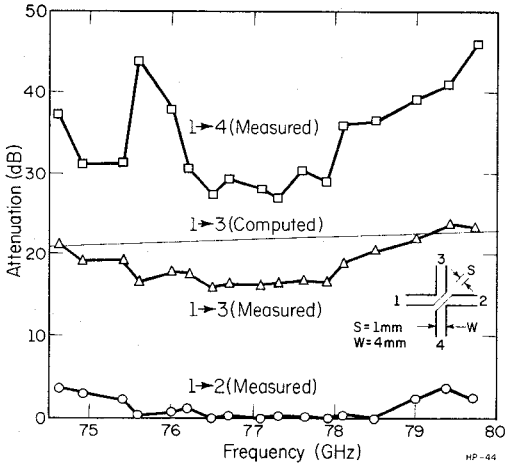

Fig. 2. Performance of the beam-splitter-type coupler.

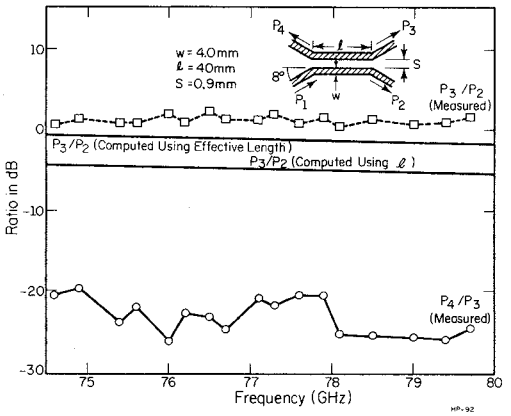

Fig. 5. Performance of the distributed-type coupler.

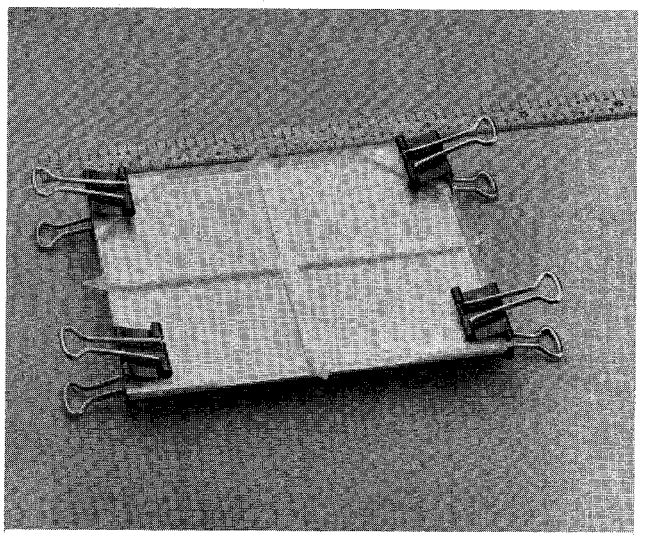

Fig. 3. Beam splitter type directional coupler.

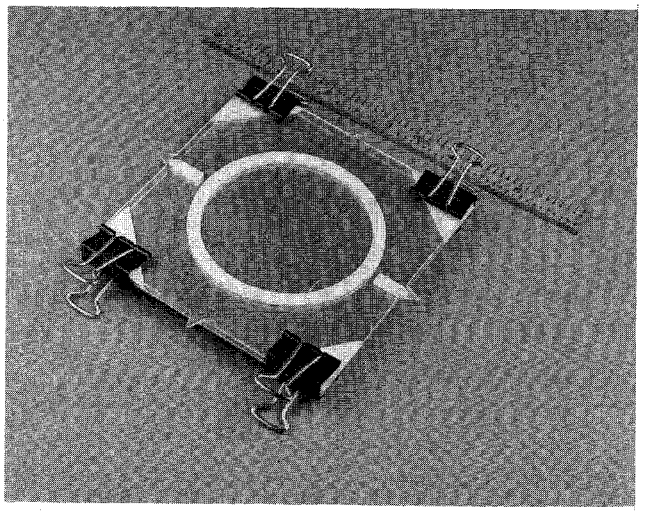

Fig. 6. Ring resonator.

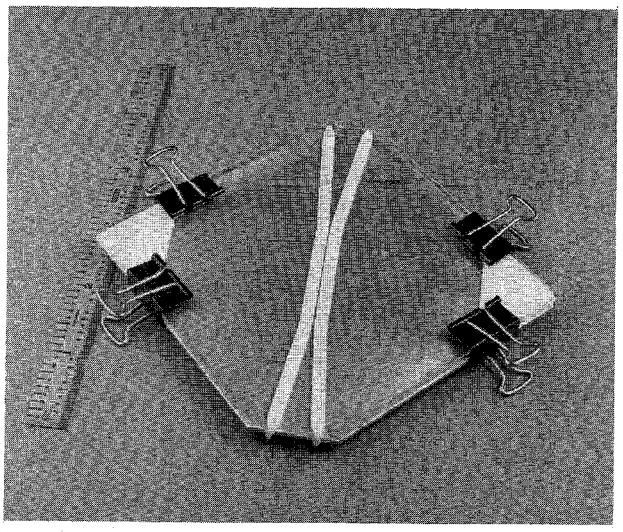

Fig. 4. Distributed-type directional coupler.

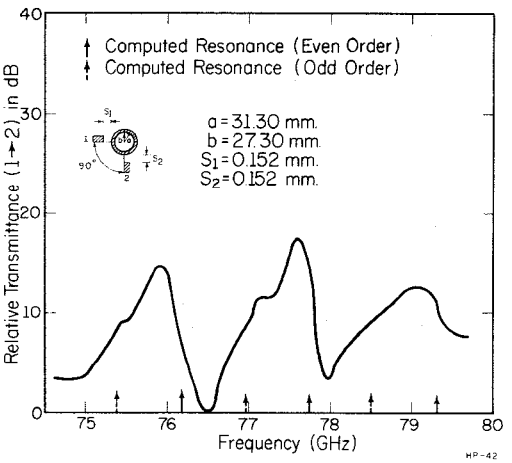

Fig. 7. Frequency characteristics of the ring resonator.